International Journal of Heat and Fluid Flow xxx (2014) xxx–xxx

Contents lists available at ScienceDirect

International Journal of Heat and Fluid Flow

journal homepage: www.elsevier.com/locate/ijhff

Hybrid simulation of wake-vortex evolution during landing on flat terrain and with plate line

Anton Stephan [a,*], Frank Holzäpfel [a], Takashi Misaka [b]

[a] Deutsches Zentrum für Luft- und Raumfahrt (DLR), Institut für Physik der Atmosphäre, 82234 Oberpfaffenhofen, Germany
[b] Tohoku University, Institute of Fluid Science, Sendai 980-8577, Japan

ARTICLE INFO

Article history:
Available online xxxx

Keywords:
Wake vortex
Spatial LES
RANS-LES coupling
End effects
Landing
Plate line

ABSTRACT

Wake-vortex evolution during approach and landing of a long range aircraft is investigated. The simulations cover final approach, touchdown on the tarmac, and the evolution of the wake after touchdown. The wake is initialized using a high fidelity Reynolds-averaged Navier–Stokes solution of the flow field around an aircraft model. The aircraft in high-lift configuration with deployed flaps and slats is swept through a ground fixed domain. The further development of the vortical wake is investigated by large-eddy simulation until final decay. The results show the formation of a pronounced shear layer at the ground and an increase in circulation in ground proximity, caused by the wing in ground effect. Disturbances at disconnected vortex ends, so-called end effects, appear after touchdown and propagate along the wake vortices against the flight direction. They lead to a circulation decay of the rolled-up wake vortices, combined with a growth of the core radius to 300% of its initial value. After touchdown wake vortices are subjected to strong three-dimensional deformations and linkings with the ground. The complete vortex evolution, including roll-up and decay, is accelerated in ground proximity. Additionally the effect of a plate line installed in front of the runway is studied with this method. The plates cause disturbances of the vortices propagating to either side and interacting with the end effects. The plate line further accelerates the vortex decay, reducing the circulation rapidly by another 25% of its initial value.

1. Introduction

As an unavoidable consequence of lift, aircraft generate a pair of counter-rotating and long-lived wake vortices that pose a potential risk to following aircraft, due to strong coherent flow structures (Gerz et al., 2002). The probability of encountering wake vortices increases significantly during final approach in ground proximity, since rebounding vortices may not leave the flight corridor vertically and the possibility of the pilot to counteract the imposed rolling moment is restricted (Critchley and Foot, 1991; Holzäpfel and Steen, 2007). In the recent "Challenges of growth 2013" report (Eurocontrol, 2013) the conceivable capacity problems of airports are elucidated. Several economic scenarios for the future European airport demands are analyzed, realizing that there will be around 1.9 million unaccommodated flights in the most-likely case, constituting approximately 12% of the demand in 2035. A reduction of the established static aircraft separation distances appears feasible employing advanced wake-vortex advisory systems (WVAS) incorporating the state-of-the-art wake-vortex physics to accurately predict vortex strength and position (Gurke and Lafferton, 1997; Hinton et al., 2000; Holzäpfel et al., 2009). However, established WVAS performance is unsatisfactory in runway proximity, as e.g. significantly less critical encounters are observed than expected (Holzäpfel et al., 2011). This means that the physical mechanisms of wake-vortex evolution and decay during and after landing are not sufficiently understood.

A landing aircraft generates a highly complex flow field in terms of structure and relevant scales. The flow around an aircraft's main wing, fuselage, slat, flap, jet engine and tail plain, as well as the interaction with the approaching ground and the sudden lift reduction during touchdown substantially affect the generated wake vortices. The evolution of the aircraft's wake in its meteorological environment is an example of complex turbulent flows, composed of strong coherent flow structures that exhibit a range of length scales spanning several orders of magnitude all interacting with one another.

In accordance with flight practice[1] we characterize the evolution of the aircraft's wake during landing by four main phases, *Final*

* Corresponding author. Tel.: +49 8153282566.
E-mail address: anton.stephan@dlr.de (A. Stephan).

[1] http://www.skybrary.aero/index.php/Landing_Flare?utm_source=SKYbrary&utm_campaign=47ff8e1e92-SKYbrary_Highlight_04_07_2013&utm_medium=email&utm_term=0_e405169b04-47ff8e1e92-264071565 date: April 23, 2014.

http://dx.doi.org/10.1016/j.ijheatfluidflow.2014.05.004
0142-727X/

approach, Flare, Touchdown and *Roll-out*. Independently from this, the aircraft wake evolution is frequently considered to consist of three distinct phases, the *roll-up phase*, the *vortex phase* and the *decay phase* (Breitsamter, 2011). Usually Reynolds-averaged Navier–Stokes (RANS) simulations are used for the flow around the aircraft and the subsequent roll-up process of the wake in the roll-up phase (Stumpf, 2005). The dynamics of wake vortices after roll-up until decay have been mainly studied by large-eddy simulations (LES) considering various atmospheric conditions like turbulence, thermal stability and wind shear (Holzäpfel et al., 2001; Misaka et al., 2012). Those studies initialize a vortex pair with a constant velocity profile along flight direction. The interaction with the ground is also simulated by initializing fully rolled-up vortices (Proctor et al., 2000; Georges et al., 2005). This approach neglects the effects of different vortex generation heights above ground and of touchdown and may not capture full three-dimensional vortex deformations appearing during ground interaction. This simplified approach for modeling the landing phase was also used by Stephan et al. (2012). The current study reveals that the simplified modeling fails to reproduce many characteristic flow features. Complementary to simulations, field measurements of real aircraft landings have also been accomplished (Holzäpfel and Steen, 2007).

With this work we aim to understand several phenomena that could not be addressed with numerical simulations so far. How does the touchdown influence wake vortex decay? Which are the effects of the flight path angle on the vortex trajectories? Can we deduce the fully three-dimensional vortex characteristics? Do vortex evolution phases change in ground proximity?

Recent developments in RANS-LES coupling enable an innovative methodology to fly a realistic aircraft through a simulation domain generating a realistic wake (Misaka et al., 2013). For this purpose, a high-fidelity steady RANS flow field is swept through the LES domain. So a spatial development of the aircraft wake is introduced in the LES. We use this approach to simulate the final approach and landing and study the physics of the wake-vortex evolution and decay. A high-lift configuration of a long range aircraft is employed to account for the landing and flare phase. Note that this approach can be viewed as a one way coupling. The changing environment, i.e. the approach of the ground is not reflected by the RANS field. The wing in ground effect is simulated just by the LES. Therefore, particular emphasis is put on the wing in ground effect to assess the accuracy of the presented method.

The first investigations on ground effect have been performed by Wieselsberger (1922) and Prandtl (1923) employing a modification of Prandtl's lifting line theory. That is, the steady case is investigated, assuming a fixed altitude above ground, wing speed, as well as angle of attack. An overview over various analytical approaches for the quantification of the wing in ground effect (WIG) can be found in Pistolesi (1937). Solutions for two- and three-dimensional wings in ground effect may be found in Widnall and Barrows (1970). Daeninck et al. (2006) investigate wake vortex roll-up in ground effect for different wing aspect ratios and span loadings at different altitudes above ground. A double elliptical chord distribution as a model for high-lift configuration is also studied. The steady wing in ground effect is modeled using Prandtl's lifting line theory. All these considerations have been purely stationary, neither the flight path angle nor flare or the changing angle of attack have been considered. Real aircraft landings are characterized by a complex coupled system of parameters like angle of attack, flight speed, flight altitude, lift coefficient, etc. Such complex coupled systems can be derived from flight measurement data (Jategaonkar, 2006). An overview of the ground effect from the system identification view can be found in (Fischenberg, 1999). In the systemic approach analytical models for lift and drag coefficients in ground effect are considered. Model parameters are identified using flight test data and are validated in simulations.

Complex vortex deformations in ground proximity like vortex linking with the ground have been observed (Proctor et al., 2000). However, the effect of these structures encountered by following aircraft is not clear. We study so called end effects, appearing after touchdown, when vortex circulation is drastically reduced, as a reason that aircraft landings are safer than expected. End effects are vortex disturbances that appear in various situations when vortex characteristics change abruptly. These disturbances propagate along the vortices and reduce the circulation (Bao and Vollmers, 2005; Moet et al., 2005). Additionally, the interaction of end effects and disturbances caused by plate lines (Stephan et al., 2013a) – a method for artificial vortex decay enhancement – is investigated with the present approach. A comparison of simulations with experiments in a water towing tank dealing with artificial decay enhancement can be found in Stephan et al. (2013b). In the meanwhile first results of flight measurement campaigns at Oberpfaffenhofen airport as well as Munich airport (Germany) confirming plate line effects as well as landing effects have been presented in Holzäpfel et al. (2014), complementing the findings in this numerical study.

The "methods" section is divided into four parts. First, the LES code is presented. Second, we explain the wake initialization technique. Third, we list the parameters of the employed long range aircraft model. Finally, the domain and boundary treatment are presented. The "results" section consists of six subsections, a presentation of general flow features, an investigation of the wing in ground effect, the analysis of end effects, of vortex topology and vortex decay, and lastly, the illustration of vortex evolution phases in ground proximity.

2. Methods

2.1. Governing equations

The LES is performed using the incompressible Navier–Stokes code.

MGLET, developed at Technische Universität München, for solving the Navier–Stokes equations and the continuity equation (Manhart, 2004)

$$\frac{\partial u_i}{\partial t}+\frac{\partial (u_i u_j)}{\partial x_j}=-\frac{1}{\rho}\frac{\partial p'}{\partial x_i}+\frac{\partial}{\partial x_j}\left((\nu+\nu_t)2S_{ij}\right), \tag{1}$$

$$\frac{\partial u_j}{\partial x_j}=0. \tag{2}$$

Here u_i represents the velocity components in three spatial directions $(i=1,2,\text{ or }3)$, $S_{ij}=(\partial u_i/\partial x_j+\partial u_j/\partial x_i)/2$ denotes the strain rate tensor, and $p\prime=p-p_0$ equals the pressure deviation from the reference state p_0. The kinematic viscosity is given as the sum of molecular viscosity ν and eddy viscosity ν_t determined by means of a Lagrangian dynamic sub-grid scale model (Meneveau et al., 1996). Eqs. (1) and (2) are solved by a finite-volume approach, using a fourth-order finite-volume compact scheme (Hokpunna and Manhart, 2010). A split-interface algorithm is used for the parallelization of the tri-diagonal system (Hokpunna, 2009) computing coefficients of the compact scheme. A third-order Runge–Kutta method is used for time integration. The simulations are performed in parallel, using a domain decomposition approach.

The recently developed concept of artificial wake vortex decay enhancement by plate lines is also pursued in this work. A respective patent has been filed under number DE 10 2011 010 147. Fig. 1 displays the arrangement of the plates in a line perpendicular to the runway. The plate line is characterized by the plate separation Δy, the height h and the plate length. The plate line is modeled by

Please cite this article in press as: Stephan, A., et al. Hybrid simulation of wake-vortex evolution during landing on flat terrain and with plate line. Int. J. Heat Fluid Flow (2014), http://dx.doi.org/10.1016/j.ijheatfluidflow.2014.05.004

introducing a drag force source term, $-F_{D,i} = -C_D|u|u_i$, to Eq. (1) with a large drag coefficient at the plate. At the ground surface of the LES domain we employ the Grötzbach-Schumann wall model that locally computes the wall shear stress τ_w instantaneously based on the logarithmic law (Grötzbach, 1987).

2.2. Wake initialization

We employ a wake initialization approach where a realistic aircraft wake is generated in an LES domain by sweeping a high-fidelity steady RANS flow field through the domain, which enables the simulation of the wake-vortex evolution from generation until final decay (Misaka et al., 2013). The simulations are performed for a long range aircraft model in high-lift configuration that has been used in ONERA's catapult facility during the European AWIATOR project. The RANS flow field serves as a forcing term of the Navier–Stokes equations in the LES. This approach might be referred to as a fortified solution algorithm (Fujii, 1995), or a nudging technique used in data assimilation (Kalnay, 2003). The resulting velocity field in the aircraft vicinity consists of the weighted sum

$$\mathbf{V} = f(y)\mathbf{V}_{\mathrm{LES}} + (1 - f(y))\mathbf{V}_{\mathrm{RANS}} \tag{3}$$

of the LES and the RANS velocity field, see Fig. 2, with a transition function

$$f(y,\alpha,\beta) = \frac{1}{2}\left[\tanh\left[\alpha\left(\frac{y}{\beta} - \frac{\beta}{y}\right)\right] + 1.0\right]. \tag{4}$$

Here α and β represent slope and wall-distance of the transition, chosen similar to the values in Misaka et al. (2013). The mapping of the RANS flow field from an unstructured, mesh refined grid to the structured LES domain is performed by a linear interpolation conducted only once before the wake initialization. First the steady RANS solution is mapped to a Cartesian grid, a so-called frame, which is mapped to the LES grid, shifted for every time step. As the frame can only be mapped at discrete grid positions of the LES grid, a sinking glide path cannot be realized by one fixed frame. For a glide path angle of 3.56 degree this would imply on an equidistant grid that the frame has to be shifted 16 grid points horizontally, while one grid point vertically, leading to steps in the initialized wake. Therefore 16 frames have to be prepared in advance, interpolating the glide path in between, leading to a smooth wake initialization. Note that the time step, constraining the calculation by the CFL number, is determined by the grid spacing and the flight speed. To achieve smaller CFL numbers, we halve the time step by doubling the number of interpolated frames. Hence, thirty-two frames of the RANS field are prepared in a preprocessing and used alternately to achieve a realistically small aircraft descent angle. This requires additional memory, however, few additional computation time is needed.

This hybrid method also enables to study the effect of an ambient turbulent crosswind on the aircraft wake by initializing the wake to a pre-simulated turbulent wind field. In the present work, turbulent wind, as well as stratification effects are not taken into account.

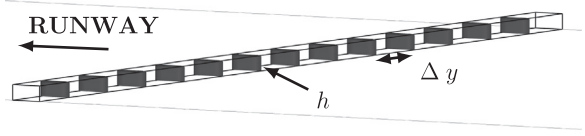

Fig. 1. Schematic representation of a plate line. Thin plates with height h and separation Δy.

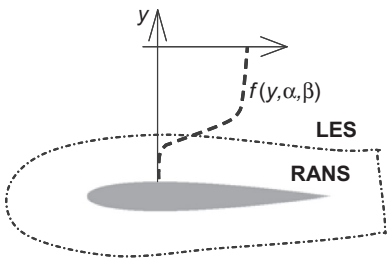

Fig. 2. Schematic of a weighting function for a combination of RANS and LES flow fields (Misaka et al., 2013).

2.3. Computational setting

We employ a RANS flow field obtained by the DLR TAU-code (Keye, 2011) from a steady compressible RANS simulation. An adaptive mesh refinement for wing-tip and flap-tip vortices, as well as the fuselage wake is employed. The flow conditions of the RANS simulation are the same as in ONERA's catapult facility experiment, i.e. chord based Reynolds number $Re = 5.2 \times 10^5$ (two orders of magnitude lower than the real aircraft flight), flight speed $U_\infty = 25$ m/s, and a lift coefficient of $C_L = 1.4$. The 1/27 scaled model has a wingspan of 2.236 m. We normalize quantities with the reference values for an elliptic load distribution (Gerz et al., 2002), initial circulation, vortex spacing, vortex descent velocity, characteristic time, vorticity unit,

$$\Gamma_0 = \frac{2C_L U_\infty b}{\pi\Lambda}, \quad b_0 = \frac{\pi}{4}b, \quad w_0 = \frac{\Gamma}{2\pi b_0}, \quad t_0 = \frac{b_0}{w_0}, \quad \omega_0 = \frac{1}{t_0}, \tag{5}$$

with a wing aspect ratio of $A_r = 9.3$. The resulting reference values for the normalization are $\Gamma_0 = 5.36\ \mathrm{m^2/s}$ for circulation, $b_0 = 1.756$ m for length, $w_0 = 0.49$ m/s for velocity, and $t_0 = 3.617$ s for time. Normalized quantities are expressed in units of the reference values in Eq. (5) and are denoted by an asterisk. We set $t = 0$ at the instant of the touchdown. The maximum tangential velocity of the wake vortices is around 10 m/s (around 30 m/s for a real aircraft).

2.4. Computational domain, approach and boundary treatment

The hybrid simulation approach and the switch to pure LES (large arrow) is sketched in Fig. 3. The first part of the simulations includes the hybrid RANS/LES wake initialization until touchdown, Fig. 3(a). The second part is a pure LES of the evolution of the aircraft wake, Fig. 3(b). We employ periodic boundary conditions in horizontal directions, a no-slip condition at the ground and a free-slip condition at the top. The aircraft starts in the back part of the domain passes the boundary and approaches the ground. Because of the periodicity the aircraft is placed in front of the domain in Fig. 3(a). After touchdown the first slice of the domain is extended into the back part at the slope of the vortex and closed artificially to a horse shoe vortex, see Fig. 3(b). This procedure effectively avoids disturbances generated at the starting point of vortex initialization. Note that wake vortex linking due to Crow instability is frequently observed in cruise altitudes and may also occur in ground proximity.

In the simulations, the aircraft approaches the ground with a flight path angle of 3.57 degree, whereas the angle of attack of the fuselage equals 5.54 degree. In addition, the aircraft surface distance parameter $\beta^* = 0.08$ is linearly reduced depending on

Please cite this article in press as: Stephan, A., et al. Hybrid simulation of wake-vortex evolution during landing on flat terrain and with plate line. Int. J. Heat Fluid Flow (2014), http://dx.doi.org/10.1016/j.ijheatfluidflow.2014.05.004

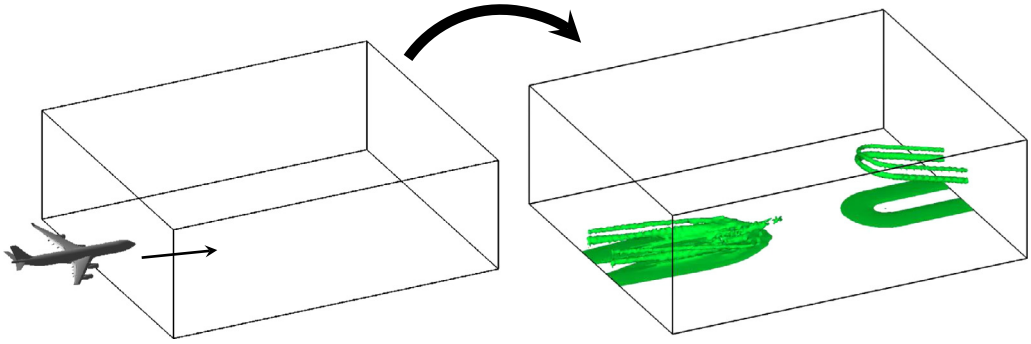

(a) Wake initialization until touchdown. (b) LES, vortex decay after touchdown.

Fig. 3. Schematic of aircraft landing displaying the computational domain and the wake evolution (a) before touchdown, during wake initialization, (b) after touchdown with artificial vortex reconnection.

the distance to the ground beneath the aircraft to $\beta^* = 0.013$. This way, in ground proximity the influence of the ground is allowed to develop freely in the LES.

When the landing gear touches the ground the lift ceases quickly. Then the bound vortex, i.e. the circulation around the aircraft wings, and consequently the wake vortices are strongly reduced. If we assume a complete disappearance of the lift, the aircraft wake can be regarded as white noise after touchdown (Hah and Lakshminarayana, 1982). We model the touchdown just by removing the RANS flow field forcing term from the simulation and disregard the white noise wake of the rolling aircraft.

In the LES we employ uniform mesh spacing for all three spatial directions, with a resolution of $dx^* = dy^* = dz^* = 0.011$, comparable to the mesh spacing in Misaka et al. (2013). Hence, the out of ground effect characteristics and behavior of the wake vortices should be similar to those described in Misaka et al. (2013). The mesh resolves the primary vortices well, while secondary vortices appearing at the ground, as well as secondary vortices in the aircraft wake are not well resolved, which might have an effect on the wake vortex evolution.

The dimensions of the complete computational domain used for wake initialization are $23.3b_0, 5.8b_0$, and $2.2b_0$ in flight, spanwise and vertical directions, respectively. After touchdown a wider domain of $8.7b_0$ is used for the simulation of the vortex decay to capture the strong divergence of the vortices. The back part of the domain with a length of $5b_0$ is used for aircraft starting and the subsequent reconnection of the vortex pair by a horseshoe vortex. In the following figures this part is not depicted. The aircraft passes the domain boundary at a height of $1.2b_0$. At touchdown the tail wing is at $x^* = 16.3$ whereas the plate line is centered at $x^* = 5.1$. The plates with lengths and heights of $0.2b_0 \times 0.1b_0$ are separated by $0.45b_0$, see Fig. 1. Two simulations are presented, with and without the influence of the plate line.

3. Results

3.1. General flow field

The wake directly behind the aircraft wings consists of a complex vorticity distribution, see Fig. 4, as well as Misaka et al. (2013). However, only a few vortices remain behind the aircraft tail, namely the wing-tip and flap-tip vortices, as well as vortices from the wing-fuselage junction, visible in Figs. 4(a) and (b). The wake vortices as well as the bound vortex along the wing induce a shear layer at the ground surface, see Fig. 4(a). The plate line is disturbing the secondary vorticity layer, see Fig. 4(b). Out of ground proximity wing-tip and flap-tip vortices merge at a distance of about $x^* = 13$ from the aircraft (Misaka et al., 2013). Note that the merger of flap-tip and wing-tip vortex to a single vortex pair is accelerated very close to the ground, see Fig. 4(c). The merging distance in ground proximity is evaluated in Section 3.5.

Shortly after touchdown the bound vortex vanishes and the free ends of the wake vortices start to interact with the vorticity layer at the ground. Levels of high vorticity magnitude dissolve starting at the point of touchdown, see Figs. 4(e) and (f). This process constitutes the end effects propagating as a combination of helical disturbances around the vortex cores and a pressure jump within the vortex cores, see Fig. 4(e). At the ground the shear layer rolls up to secondary vortex structures, which separate from the ground and wrap around the primary vortices, see Figs. 4(g) and (h). Depending on the vortex generation altitude above the ground this process starts first at the point of touchdown and is initiated locally above the plate line. Port- and starboard-vortices are no longer linked by the bound vortex and quickly diverge at the point of touchdown, see Figs. 4(c)–(f). Additionally we observe linking of the vortex ends with the ground, see Fig. 4(h). At the plate line secondary vortex structures wind around the primary vortices and propagate by self-induction in axial directions to either sides (Stephan et al., 2013a). These helical disturbances finally interact with the end effects and thus effectively reduce circulation strength all along the final approach area.

The turbulent wake generated by the fuselage, Figs. 4(a) and (b), is stretched around the primary vortices and is quickly transported to the ground between the vortex pair, disturbing the relatively smooth shape of the secondary vorticity layer at the ground surface, Figs. 4(b)–(d). As a consequence, the secondary vortices are disturbed and are themselves generating irregularities. The counter-rotating secondary vortices finally develop into relatively strong turbulent structures initiating rapid vortex decay of the primary vortices (Stephan et al., 2013a).

3.2. Wing in ground effect

In ground proximity the presence of a fixed surface significantly modifies aerodynamics. Close to the ground the downwash is limited by the rigid ground surface. This results in a number of physical phenomena arising in ground proximity summarized as "wing in ground effect". The effect appears, in general, for wing altitudes lower than a wing span above ground and has a crucial consequences for the landing. The main phenomena resulting from the ground effect are (Etkin, 1972)

1. the pressure below the wings increases,
2. the sink rate is reduced,
3. reduced downwash angle at the tail,

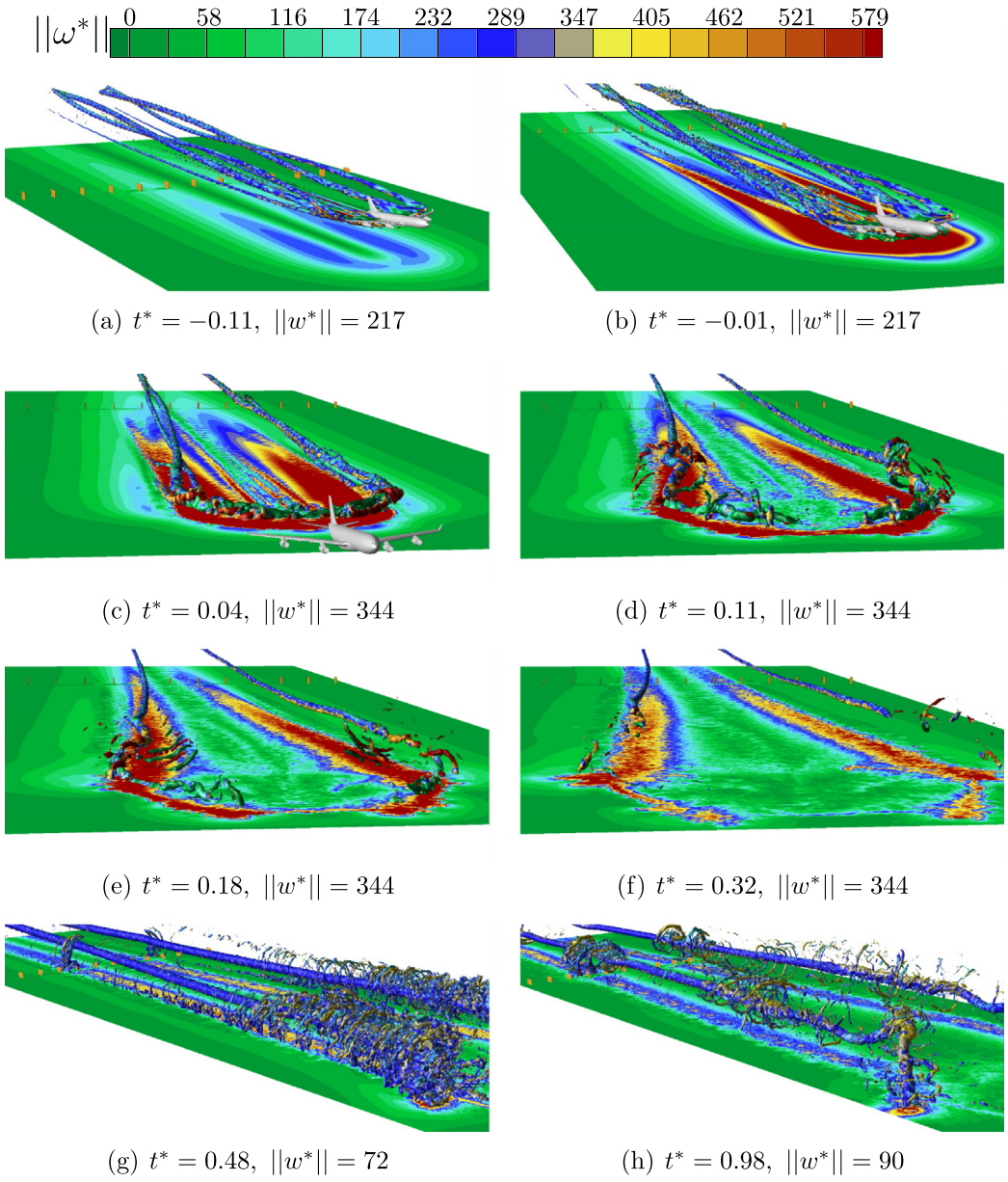

Fig. 4. Aircraft landing with roll-up, approach, touchdown, developing end effects, and influence of a plate line. Different perspectives and levels of vorticity iso-surface, ground colored with vorticity magnitude. (For interpretation of the references to colour in this figure legend, the reader is referred to the web version of this article.)

4. increase in the lift,
5. reduction in the induced drag.

Here we are particularly interested in the strength, i.e. circulation, of the wake vortices. The total lift force can be computed from the circulation distribution over the aircraft wings $\Gamma(y)$ and the aircraft speed U (e.g. Kundu and Cohen, 1990)

$$L = \int_{-b/2}^{b/2} \rho U \Gamma dy. \tag{6}$$

Assuming a balance of the lift and weight force $L = Mg$, where M denotes the aircraft mass and g denotes the gravitational acceleration, the lift is approximately constant. It is known that a real aircraft reduces its speed before landing, during flare. Hence, the integral value of the circulation distribution increases accordingly. Assuming a uniform increase of the wing load we conclude that the root circulation Γ_0 also increases, which can be assumed to be the total wake vortex strength for a at least small period of time, due to Kelvin's circulation theorem (Kundu and Cohen, 1990). We may conclude: If we assume a nearly constant lift force L balancing the weight forces, the wake vortex circulation Γ_0 increases corresponding to the decrease of U, by Eq. (6). Because in reality the sink rate of the aircraft is also reduced prior to touchdown a further increase of the circulation appears, which is realized by an increase of the angle of attack.

We observe a strongly pronounced wing in ground effect in the simulations. The fading RANS field beneath the aircraft allows the pressure field to develop between the aircraft and the ground surface, see Fig. 5. The left side depicts a pressure iso-surface and reveals the pressure pillow beneath the aircraft and the aircraft nose. During approach to the ground the belly pillow grows. On the right side the contours show the quantitative growth of the pressure in the center plane beneath the aircraft. Hence, we are able to reproduce the theoretically stated ground effect with our LES/RANS approach. In the simulations, so far, we do neither

Please cite this article in press as: Stephan, A., et al. Hybrid simulation of wake-vortex evolution during landing on flat terrain and with plate line. Int. J. Heat Fluid Flow (2014), http://dx.doi.org/10.1016/j.ijheatfluidflow.2014.05.004

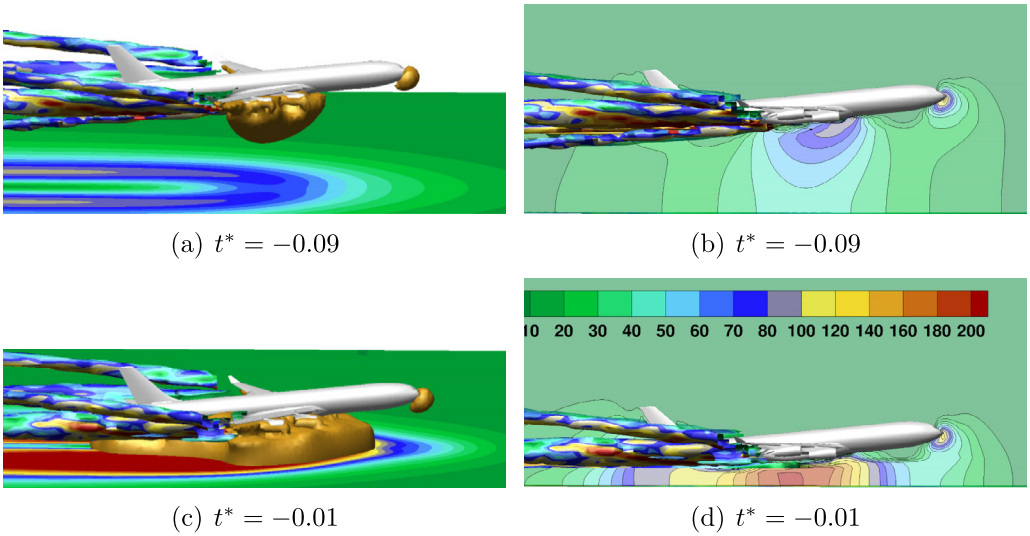

(a) $t^* = -0.09$ (b) $t^* = -0.09$

(c) $t^* = -0.01$ (d) $t^* = -0.01$

Fig. 5. Pressure increase in ground proximity, pressure iso-surface $p = 60$ N/m^2 (left), pressure distribution in center plane (right). Vorticity magnitude visualizing the ground surface (left) and the wake (both sides).

reduce the flight speed nor modify the angle of attack during flare. Note, there is no response of the aircraft towards the lift increase in ground proximity.

Fig. 6 shows the circulation distribution along the flight track at the instant of touchdown. The ground effect is manifested by the increase of circulation towards lower flight altitudes. In addition theoretical results from Daeninck et al. (2006) are plotted, normalized by the initial circulation of the LES. These assume a double-elliptic wing with an aspect ratio $A_r = b/c = 10.0$, which was used as a typical case for modern commercial airplanes. Qualitatively the curves agree, but the theoretically stated increase of the wake vortex strength is clearly exceeded by the LES simulations, which possibly can be explained by an additional pressure increase due to aircraft descent. Further, the theoretical considerations neglect viscosity. Indeed, due to viscosity the bound vortex creates a vorticity layer at the ground, see Fig. 5 (left), which results in an additional pressure increase beneath the aircraft. These considerations indicate that for a highly accurate simulation of the flare, a transient two way coupled RANS/LES method, fully accounting for the ground surface, would be required.

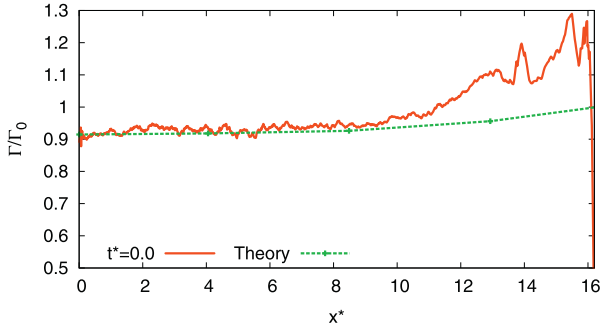

Fig. 6. Circulation distribution at the instant of touchdown, comparison with theoretical results from Daeninck et al. (2006).

3.3. End effects

The disconnected vortices dissolve starting from the point of touchdown as vortices may not end freely in space in accordance with the Helmholtz vortex theorems (Kundu and Cohen, 1990). Inside the vortex core the low pressure region is faced with the high pressure region at the end of the disintegrated vortex. The pressure difference causes strong axial flows and disturbances such that the vortices start to dissolve, see Fig. 7(a) and (c). This phenomenon is called end effect. Together with an increase of pressure we observe helical disturbances around the vortex cores propagating against the flight direction. The reduction of circulation coincides with an increase of the core radius, see Section 3.5. Note that the primary vortices quickly link with the ground leading to a stabilization of the primary vortices, preventing them from further dissolving and thus conserving a certain level of circulation. In addition, the classical interaction of the wake vortices with the ground proceeds, i.e. secondary vortex structures separate from the ground and wrap around the primary vortices, see Fig. 7(b) and (d). This type of ground effect, also observable in temporal LES, is independent of the end effects and depends only on the altitude of the vortices. The lower the flight height the earlier and more rapid the ground effect sequence proceeds. Hence, the propagation speed of the end effects and the ground effect do not coincide, see Fig. 7.

End effects can occasionally be observed when condensation trails form in humid air marking the vortex cores that adopt helical shapes and quickly disappear after touchdown.[2] Condensation trails may occur when the temperature, lowered by the pressure decrease in the vortex core, leads to supersaturation of water vapor and thus to condensation. So the rapid disappearance of the condensation trail is directly related to the pressure and consequential temperature increase in the vortex cores.

3.4. Vortex divergence and topology

After touchdown wake vortices are abruptly cut off. They are neither connected by the bound vortex nor to the very weak wake of the braking aircraft, see Fig. 4. Wake vortices inherently diverge in ground proximity. The divergence is not uniform, but is mostly pronounced at the point of touchdown and proceeds against the flight direction, as depicted in Fig. 8(a). At $t^* = 2.22$ a maximum vortex separation of more than $7b_0$ is reached. In the LES a lateral

[2] Videos available online at http://www.youtube.com/watch?v = oHGqxM1-rAI, http://www.youtube.com/watch?v = PpUftG_mxg8, and http://www.youtube.com/watch?v = KqU70RORXtA [retrieved November 2013].

Please cite this article in press as: Stephan, A., et al. Hybrid simulation of wake-vortex evolution during landing on flat terrain and with plate line. Int. J. Heat Fluid Flow (2014), http://dx.doi.org/10.1016/j.ijheatfluidflow.2014.05.004

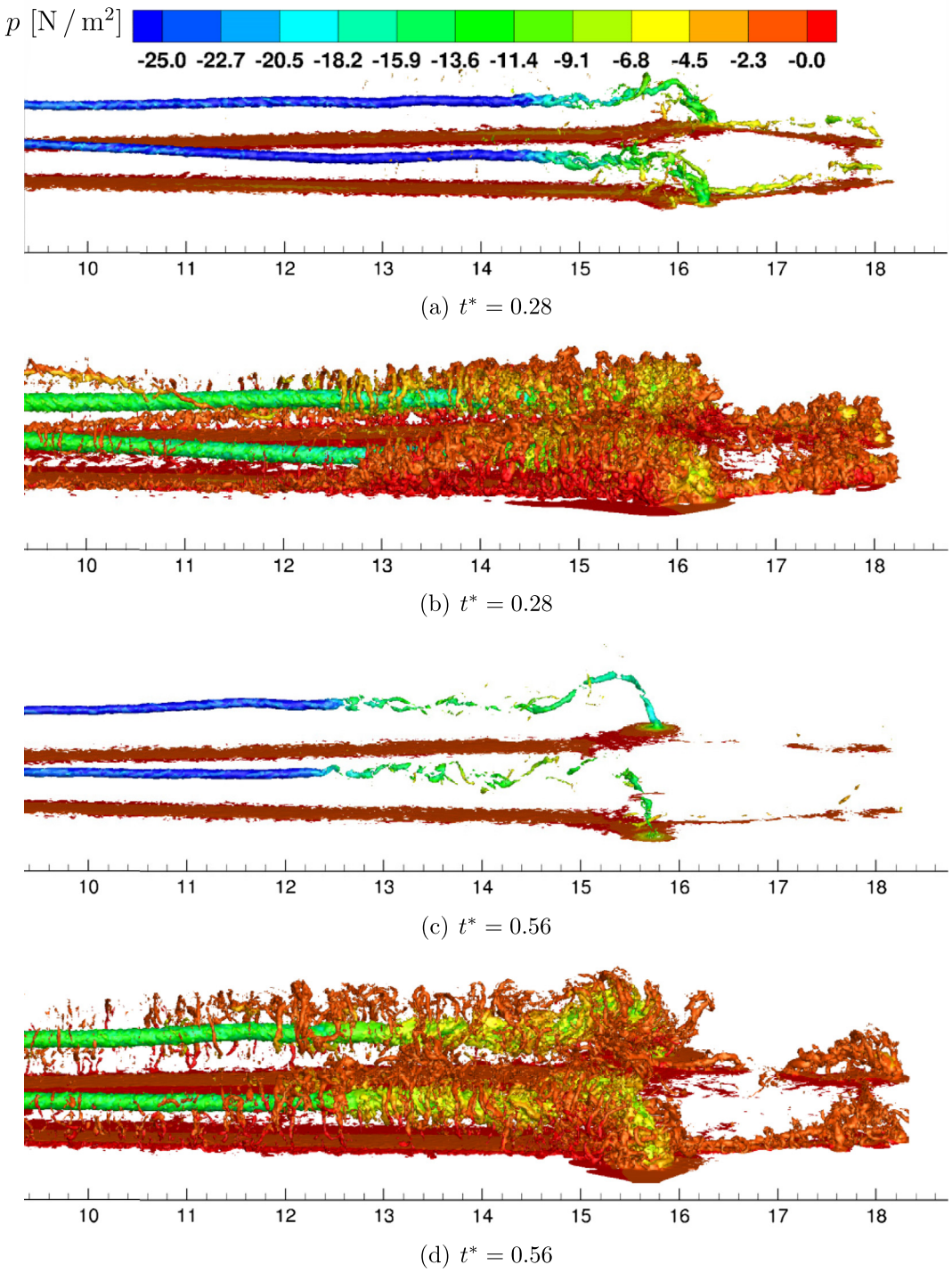

Fig. 7. Iso-vorticity surface $||\omega^*|| = 235$ (a) and (c) and $||\omega^*|| = 76$ (b) and (d), colored by pressure showing end effects as pressure disturbance and helical disturbances of the vortex core as well as ground effect for different time steps. (For interpretation of the references to colour in this figure legend, the reader is referred to the web version of this article.)

domain width of $8.6b_0$ is employed, which does not completely cover the observed divergence. Later, close to the periodic lateral domain boundaries, the vortices even connect across the boundaries, hence we may expect even larger vortex separations close to the touchdown area in reality.

The wake vortex topology in ground proximity features pronounced three-dimensional characteristics. Fig. 8(b) shows the complex development of the vortices after touchdown. Beside the non-uniform divergence, the rebound is non-uniform as well, in strong contrast to temporal LES (Stephan et al., 2013a). As the rebound is driven by secondary vortices, which are generated first at low flight altitudes, the rebound starts close to the touchdown zone. The secondary vortices, winding around the primary vortices, the end effects, and the ground linking deform the primary vortices to helical structures. Close to touchdown we even observe multiple vortex linking with the ground, as vortex parts, that come close to the ground, tend to reconnect with the ground, or equivalently formulated, with their image vortices. The free vortex ends, connected

Please cite this article in press as: Stephan, A., et al. Hybrid simulation of wake-vortex evolution during landing on flat terrain and with plate line. Int. J. Heat Fluid Flow (2014), http://dx.doi.org/10.1016/j.ijheatfluidflow.2014.05.004

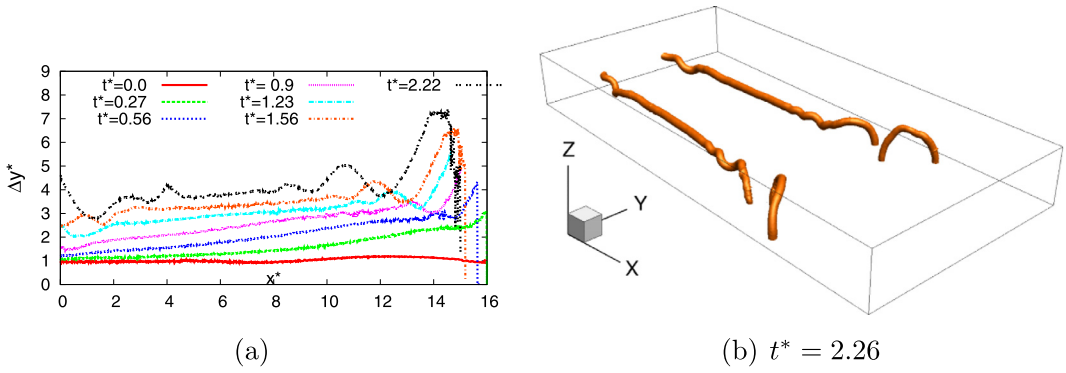

Fig. 8. (a) Lateral vortex spacing at different vortex ages, (b) multiple ground linkings after touchdown, visualized by iso-surface of pressure.

with the ground, move against the flight direction, i.e. the helices contract. Such a complex behavior is not known from classical temporal LES but might correspond to reality. Indeed, vortex linking with the ground has been observed in reality (Proctor et al., 2000). An evaluation in single slices, perpendicular to flight direction, commonly performed in flight measurements, would display the shift of that helix corresponding to peaks and kinks of the vortex altitude.

3.5. Vortex decay and core radius

Of particular interest is the vortex strength that ultimately might affect a following aircraft. As a common measure of the vortex intensity for aircraft with sufficiently large wingspans, we consider $\Gamma_{5-15} = 0.1 \int_{5m}^{15m} \Gamma(r)dr$ for the primary vortices, where $\Gamma(r) = \oint \vec{u} \cdot d\vec{s}$ denotes the circulation around a circle of radius r centered in the vortex core (Holzäpfel et al., 2003). For circulation evaluation of the aircraft wake we take the center of the flap-tip vortex. Misaka et al. (2013) evaluate Γ_{5-15} for wing-tip as well as flap-tip vortex. They find that out of ground the circulation Γ_{5-15}, centered at the flap-tip vortex, as well as the finally rolled-up vortex, is slightly larger than $0.9\Gamma_0$.

At the instant of touchdown ($t^* = 0$) the circulation is increasing from $0.9\Gamma_0$ at out of ground altitudes towards the ground, as detailed in Section 3.2, see Fig. 9. The end effects after touchdown lead to a rapid circulation decay starting from the very ends of the wake vortices. The disturbance propagates throughout the full domain. In the case without a plate line the decay proceeds quite uniformly.

The effect of the plate line is clearly visible in Fig. 9 (right). Above the plate line, at $x^* = 5.1$, the circulation decay is initiated propagating subsequently to either side. The disturbances from the end effects as well as from the plate line superpose, leading to a more vigorous decay. In the region of the plate line we have a reduction of the circulation to less than 50% at $t^* = 2.2$, whereas without the plate line the circulation falls to only 70%. Note that the investigated angle of approach of 3.56 degree is to high compared to 3 degree as a standard in aviation. As a consequence the effect of the plate line should be even more pronounced at an airport.

The core radius, increases drastically after touchdown to 300% of its initial value. Note that the interaction of the end effect and the disturbance from the plate line leads to intriguing behavior of the core radius. In contrast to the case without a plate line, where the vortex bursting propagates, the growth of the core radius is suppressed in the region of the plate line (orange line). The end effects propagate with an approximately constant speed of $U^*_{prop} = 7.1$ up to a time of $t^* = 2$.

3.6. Vortex evolution phases in ground proximity

Out of ground proximity the three vortex evolution phases, the *roll-up phase*, the *vortex phase* and the *decay phase* depend mainly on the meteorological conditions and proceed uniformly along

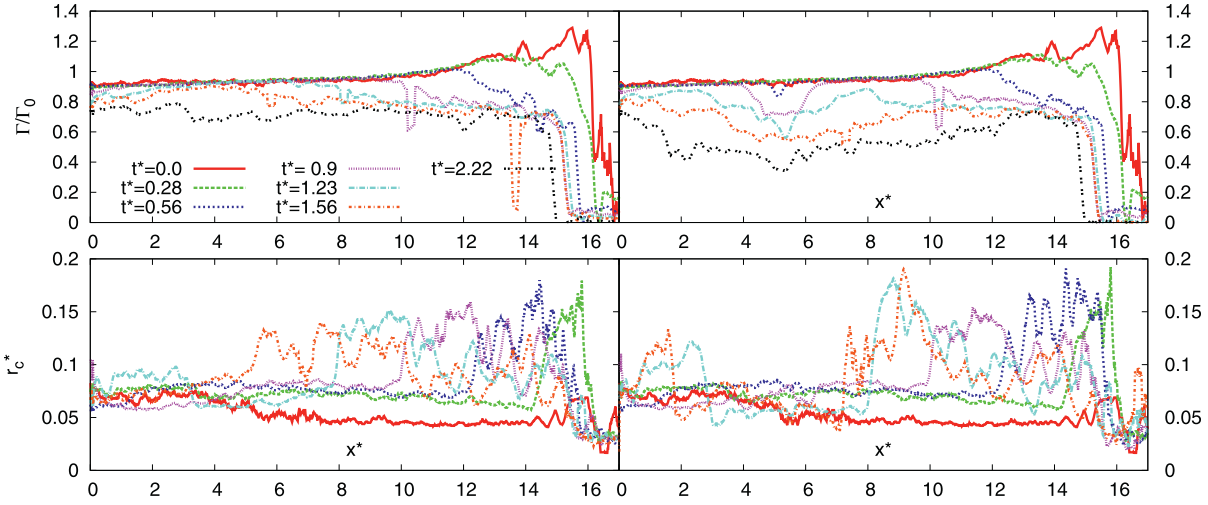

Fig. 9. Vortex circulation (Γ_{5-15}) distribution and core radius evolution no plate line (left), plate line (right), ($t^* = 2.22$ only in circulation plots).

Please cite this article in press as: Stephan, A., et al. Hybrid simulation of wake-vortex evolution during landing on flat terrain and with plate line. Int. J. Heat Fluid Flow (2014), http://dx.doi.org/10.1016/j.ijheatfluidflow.2014.05.004

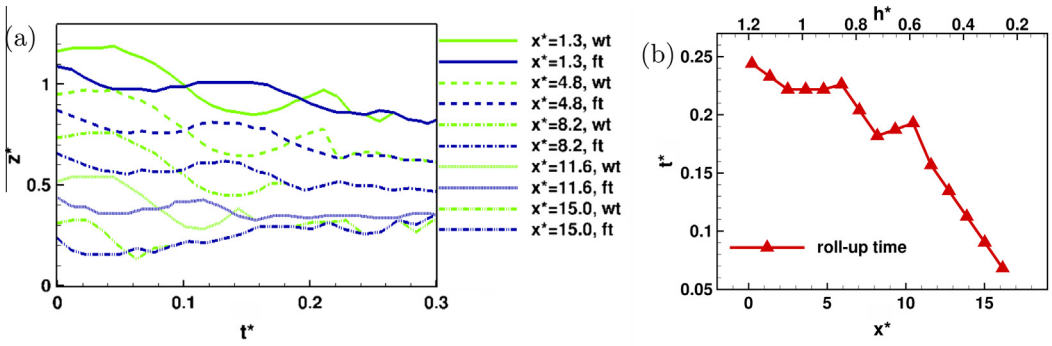

Fig. 10. Roll-up of wing-tip (wt) and flap-tip (ft) vortex. (a) Altitude of vortices at different positions plotted until roll-up against time. (b) Vortex roll-up time depending on vortex generation height h^*.

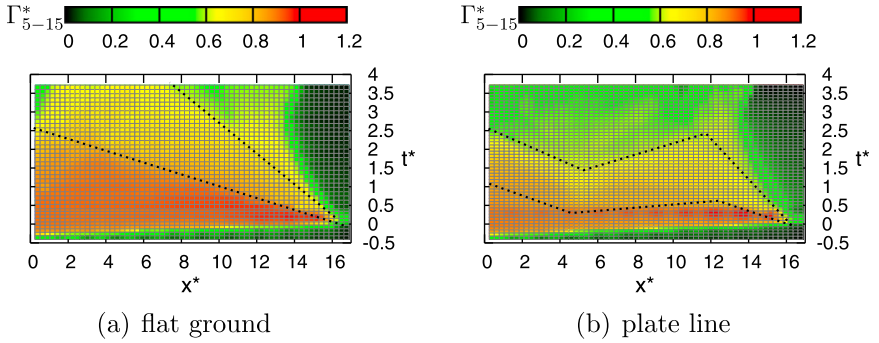

Fig. 11. Vortex circulation (Γ_{5-15}/Γ_0) distribution (color coded), schematically showing phases of vortex decay by color and dashed line. (For interpretation of the references to colour in this figure legend, the reader is referred to the web version of this article.)

the flight path (Breitsamter, 2011). This crucially changes in ground proximity.

The roll-up phase is accelerated, depending on the generation altitude of the aircraft wake. Fig. 10(a) depicts the roll-up process of the wing-tip and flap-tip vortex in different slices perpendicular to flight direction. The two vortices are seen to alternate in their z^* positions as they roll up, until they merge into a single vortex. Out of ground proximity, in accordance with Misaka et al. (2013), the roll-up is completed after approximately $t^* = 0.25$. Closer to the ground the distance between wing-tip and flap-tip vortex is progressively reduced, due to the influence of the ground surface. Fig. 10(b) depicts the roll-up time depending on the generation altitude. Note that the roll-up time decreases progressively.

In ground proximity also the wake vortex decay phases depend on aircraft altitude. Due to end effects and ground proximity the vortex decay is strongly accelerated close to touchdown zone. To visualize the decay phases Fig. 11 shows the vortex circulation (color coded) against position and time. We roughly assign the roll-up phase to a circulation larger than $0.9\Gamma_0$ (red), the vortex phase to $0.65\Gamma_0 < \Gamma < 0.9\Gamma_0$ (yellow), and the decay phase to a circulation lower than $0.65\Gamma_0$ (green). Fig. 11(a) depicts landing with flat ground. At time $t^* = 0$ the touchdown takes place. At negative times the wake is initialized starting at $x^* = 0$, the domain boundary, and then shifted according to the flight speed. Out of ground proximity the decay proceeds uniformly, i.e. the color coded pattern would have a parallelogram shape. In contrast, a triangular shape describes the decay characteristics during landing, schematically shown in Fig. 11(a). The end effect and the flight height dependent ground effect accelerate the decay and propagate against the flight direction with an approximately constant speed. The effect of a plate line on the decay phases changes the characteristics, see Fig. 11(b). The plate line additionally shortens the vortex phase and rapidly initiates the decay phase leading to an irregular pattern.

4. Conclusion

A complete landing phase of a long range aircraft including final approach, flare, touchdown, and the evolution of its wake is simulated, combining RANS and LES flow fields. A series of 32 frames of one steady RANS solution is used alternately as a forcing term in the ground fixed LES domain. The aircraft model in high-lift configuration with flaps and slats deployed, is swept through the domain at a descent angle of 3.56 degree. After initialization of the wake, the free vortex ends are artificially closed by a "horse shoe", to avoid end effects from the starting point. An equidistant Cartesian mesh is employed in all three spatial directions. Hence, the flow close to the ground is not well-resolved but modeled employing a wall model.

The complex multi-scale flow field of a landing aircraft, particularly the different vortices constituting the wake are visualized and analyzed. In the LES we observe a pronounced increase of circulation, caused by the wing in ground effect, exceeding theoretical stationary considerations. Since the landing process is approximated by one steady RANS field, the flare as well as the instant of touchdown are approximated by an adaptation of the transition function between the RANS field and the freely evolving LES. A thorough treatment of flare and touchdown would require a two way coupling of the LES and the RANS solver. It is planned to employ a series aircraft flows generated by a transient simulation (URANS) of the landing in future. End effects occurring after

Please cite this article in press as: Stephan, A., et al. Hybrid simulation of wake-vortex evolution during landing on flat terrain and with plate line. Int. J. Heat Fluid Flow (2014), http://dx.doi.org/10.1016/j.ijheatfluidflow.2014.05.004

touchdown are investigated in detail. They lead to rapid circulation decay combined with core radius growth. The interaction of the primary wake vortices with the vorticity layer induced at the ground also starts at the point of touchdown and proceeds against the flight direction. In ground proximity wake vortices are subjected to strong deformation and transport. Substantial vortex separation distances are observed at the touchdown zone connected with multiple vortex linkings.

The distinct vortex evolution phases are shortened in ground proximity. The merger of wing-tip and flap-tip vortex is accelerated by up to four times, depending on the generation altitude. Vortex decay is also significantly accelerated due to vigorous interaction with the ground surface, linking with the ground, as well as end effects. In addition the effect of a plate line installed in front of the runway is investigated. Rapid circulation reduction demonstrates the benefits of plate lines at airports. The combination of increased decay rates caused by end effects and the plate line enable the enhancement of flight safety in the flight phase, where most encounters occur. The employed Reynolds number of the model is two orders of magnitude below that of the corresponding original long range aircraft. To prove the described effects a comparison with field measurement campaigns is mandatory.

Acknowledgments

We would like to thank Stefan Melber (Institut für Aerodynamik und Strömungstechnik, DLR-Braunschweig) for providing the RANS data of the AWIATOR long range aircraft model. We also acknowledge Airbus for the allowance to use it. We thank Michael Manhart and Florian Schwertfirm for the provision of the original version of the LES code MGLET. Computer time provided by Leibniz-Rechenzentrum (LRZ) is greatly acknowledged.

References

Bao, F., Vollmers, H., 2005. Alleviation of end-effects in facilities for far wake investigations. In: AIAA-Paper 2005-0907, 43rd AIAA Aerospace Sciences Meeting and Exhibit, Reno, Nevada.

Breitsamter, C., 2011. Wake vortex characteristics of transport aircraft. Prog. Aerospace Sci. 47, 89–134.

Critchley, J., Foot, P., 1991. UK CAA wake vortex database: analysis of incidents reported between 1982 and 1990. Civil Aviation Authority, CAA Paper 91.

Daeninck, G., Desenfans, O., Winckelmans, G., 2006. FAR-Wake Technical Report 3.1.1-1, Span loading variations and wake roll-up in ground effect. Technical Report, Université catholique de Louvain (UCL).

Etkin, B., 1972. Dynamics of Atmospheric Flight. John Wiley & Sons, New York.

Eurocontrol, 2013. Challenges of growth. Technical Report, Summary Report.

Fischenberg, D., 1999. Ground effect modeling using a hybrid approach of inverse simulation and system identification. In: AIAA Paper 99-4324.

Fujii, K., 1995. Unified zonal method based on the fortified solution algorithm. J. Comput. Phys. 118, 92–108.

Georges, L., Geuzaine, P., Duponchel, M., Bricteux, L., Lonfils, T., Winckelmans, G., Giovannini, A., 2005. Technical Report 3.1.1-3, LES of two-vortex system in ground effect with and without wind. Technical Report, Université catholique de Louvain (UCL), Institut de Mécanique des Fluides de Toulouse (IMFT).

Gerz, T., Holzäpfel, F., Darracq, D., 2002. Commercial aircraft wake vortices. Prog. Aerospace Sci. 38, 181–208.

Grötzbach, G., 1987. Direct numerical and large eddy simulations of turbulent channel flows. In: Cheremisinoff, N. (Ed.) Encyclopedia of Fluid Mechanics. West Orange, NJ.

Gurke, T., Lafferton, H., 1997. The development of the wake vortex warning system for frankfurt airport: theory and implementation. Air Traffic Control Quarterly 5.

Hah, C., Lakshminarayana, B., 1982. Measurement and prediction of mean velocity and turbulence structure in the near wake of an airfoil. J. Fluid Mech. 115, 251–282.

Hinton, D., Charnock, J., Bagwell, D., 2000. Design of an aircraft vortex spacing system for airport capacity improvement. In: 38th AIAA Aerospace Science Meeting and Exhibit, Reno, NV, USA.

Hokpunna, A., 2009. Compact Fourth-order Scheme for Numerical Simulations of Navier–Stokes Equations. Ph.D. thesis, Technische Universität München (Germany).

Hokpunna, A., Manhart, M., 2010. Compact fourth-order finite volume method for numerical solutions of Navier–Stokes equations on staggered grids. J. Comput. Phys. 229, 7545–7570.

Holzäpfel, F., Dengler, K., Gerz, T., Schwarz, C., 2011. Prediction of dynamic pairwise wake vortex separations for approach and landing. In: 3rd AIAA Atmospheric Space Environments Conference, Honululu, Hawaii.

Holzäpfel, F., Gerz, T., Baumann, R., 2001. The turbulent decay of trailing vortex pairs in stably stratified environments. Aerospace Sci. Technol. 5, 95–108.

Holzäpfel, F., Gerz, T., Frech, M., Tafferner, A., Köpp, F., Smalikho, I., Rahm, S., Hahn, K.U., Schwarz, C., 2009. The turbulent decay of trailing vortex pairs in stably stratified environments. Air Traffic Control Quart. 17 (4), 301–322.

Holzäpfel, F., Gerz, T., Köpp, F., Stumpf, E., Harris, M., Young, R.I., Dolphi-Bouteyre, A., 2003. Strategies for circulation evaluation of aircraft wake vortices measured by lidar. J. Atmos. Oceanic Technol. 20 (8), 1183–1195.

Holzäpfel, F., Steen, M., 2007. Aircraft wake-vortex evolution in ground proximity: analysis and parametrization. AIAA J. 45, 218–227.

Holzäpfel, F., Stephan, A., Körner, S., Misaka, T., 2014. Wake vortex evolution during approach and landing with and without plate lines. In: 52nd Aerospace Sciences Meeting, National Harbor, Maryland.

Jategaonkar, R.V., 2006. Flight Vehicle System Identification. Progress in Astronautics and Aeronautics.

Kalnay, E., 2003. Atmospheric Modeling. Data Assimilation and Predictability. Cambridge University Press.

Keye, S., 2011. Fluid-structure coupled analysis of a transport aircraft and flight-test validation. J. Aircraft 48, 381–390.

Kundu, P.K., Cohen, I.M., 1990. Fluid Mechanics. Academic Press.

Manhart, M., 2004. A zonal grid algorithm for dns of turbulent boundary layer. Comput. Fluids 33, 435–461.

Meneveau, C., Lund, T.S., Cabot, W.H., 1996. A lagrangian dynamic subgrid-scale model of turbulence. J. Fluid Mech. 319, 353–385.

Misaka, T., Holzäpfel, F., Gerz, T., 2013. Wake evolution of high-lift configuration from roll-up to vortex decay. In: AIAA Paper 2013-0362, 51st AIAA Aerospace Sciences Meeting, Grapevine, Texas, USA.

Misaka, T., Holzäpfel, F., Hennemann, I., Gerz, T., Manhart, M., Schwertfirm, F., 2012. Vortex bursting and tracer transport of a counter-rotating vortex pair. Phys. Fluids 24, 025104-1–025104-21.

Moet, H., Laporte, F., Chevalier, G., Poinsot, T., 2005. Wave propagation in vortices and vortex bursting. Phys. Fluids 17, 054109.

Pistolesi, E., 1937. Ground Effect – Theory and Practice, Technical Memorandum no. 828. Technical Report, National Advisory Committee for Aeronautics, Washington.

Prandtl, L., 1923. Der induzierte Widerstand von Mehrdackern. Technical Report, Ergebnisse der Aerodynamischen Versuchsanstallt Göttingen, II, Lieferung.

Proctor, F.H., Hamilton, D.W., Han, J., 2000. Wake vortex transport and decay in ground effect: Vortex linking with the ground. In: AIAA, 2000-0757, 38th Aerospace Sciences Meeting & Exhibit, Reno.

Stephan, A., Holzäpfel, F., Misaka, T., 2012. Aircraft wake vortex decay in ground proximity – physical mechanisms and artificial enhancement. In: AIAA-Paper 2012-2672-285, 4th AIAA Atmospheric and Space Environments Conference, New Orleans (Louisiana).

Stephan, A., Holzäpfel, F., Misaka, T., 2013a. Aircraft wake vortex decay in ground proximity – physical mechanisms and artificial enhancement. J. Aircraft 50, 1250–1260, Doi: http://arc.aiaa.org/doi/abs/10.2514/1.C032179.

Stephan, A., Holzäpfel, F., Misaka, T., Geisler, R., Konrath, R., 2013b. Enhancement of aircraft wake vortex decay in ground proximity – experiment versus simulation. CEAS Aeronaut. J. (Accessed 30.11.13), doi:http://www.springerlink.com/openurl.asp?genre=article&id=doi:10.1007/s13272-013-0094-8.

Stumpf, E., 2005. Study of four-vortex aircraft wakes and layout of corresponding aircraft configurations. J. Aircraft 42, 722–730.

Widnall, S., Barrows, T.M., 1970. An analytic solution for two- and three-dimensional wings in ground effect. J. Fluid Mech. 41, 769–792, part 4.

Wieselsberger, C., 1922. Wing resistance near the ground. NACA TM-77 77.

Please cite this article in press as: Stephan, A., et al. Hybrid simulation of wake-vortex evolution during landing on flat terrain and with plate line. Int. J. Heat Fluid Flow (2014), http://dx.doi.org/10.1016/j.ijheatfluidflow.2014.05.004